CHEMISTRY
A EUROPEAN JOURNAL

FULL PAPER

DOI: 10.1002/chem.200600312

Self-organization of chiral oligothiophenes in cast film: enantiopure and racemic DACH di-amino-bis(bithiophene)

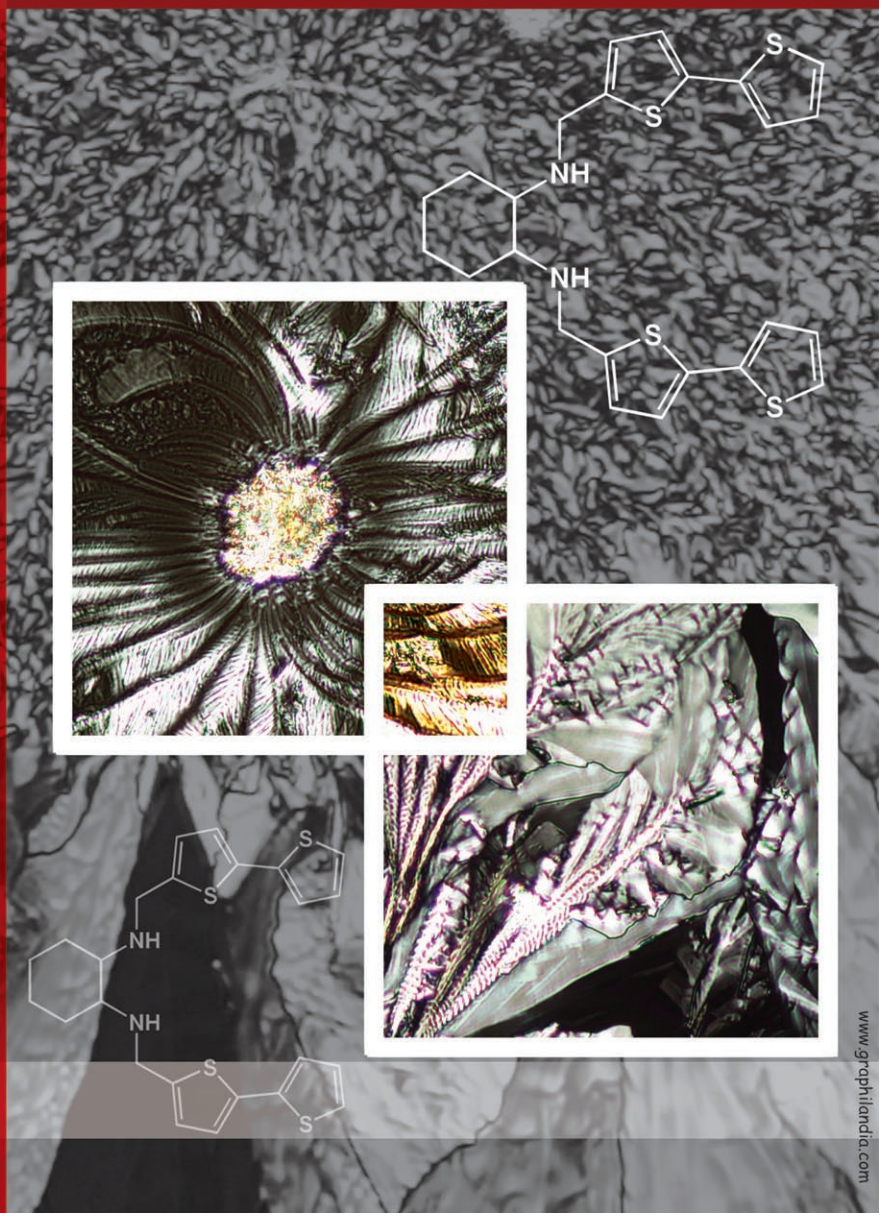

Synthesis, Multiphase Characterization, and Helicity Control in Chiral DACH-Linked Oligothiophenes**

Manuela Melucci,*[a] Giovanna Barbarella,[a] Massimo Gazzano,[a] Massimiliano Cavallini,[b] Fabio Biscarini,[b] Alessandro Bongini,[c] Fabio Piccinelli,[c] Magda Monari,[c] Marco Bandini,[c] Achille Umani-Ronchi,[c] and Paolo Biscarini[d]

Abstract: A new class of chiral oligothiophenes is described. Mono-, bi-, ter-, and quarterthiophenes have been linked to enantiopure *trans*-1,2-cyclohexanediamine (DACH) via diamino or diimino moieties. The stereochemistry of DACH, the type of linker, and oligothiophene size determine the conformational flexibility of these molecules and consequently their molecular and supramolecular helicity in solution and in the solid state. The case of diaminobis(bithiophene), which inverts helicity and shows chiral amplification in the transition from solution to film, is described in detail. Based on the combined use of circular dichroism in solution and in the solid state, single-crystal/thin-film X-ray diffraction, and polarized optical microscopy, a working mechanism has been proposed to explain this unexpected behavior.

Keywords: chirality · helical structures · oligothiophenes · self-assembly · thin films

Introduction

Oligothiophenes are multifunctional materials of great interest in organic electronics.[1] Their molecular organization and morphology in thin films control charge transport and light emission properties in technological devices.[2] Several processing approaches ranging from organic molecular beam deposition[3] to solution casting, nanopatterning,[4] and mechanical manipulation[5] have been proposed to control their thin-film organization across multiple length scales. The mechanism of self-assembly and the kinetics of growth depend on a subtle interplay between intrinsic molecular constraints and numerous noncovalent interactions such as van der Waals interactions, weak hydrogen bonds, S–S interactions, and π–π stacking.[6] Recently, the self-organizing behavior of chiral conjugated molecules in solution[7] and at surfaces[8] has attracted a great deal of interest.[9] Concerning oligothiophenes, Leclère et al. have studied the self-assembly of two enantiomeric sexithiophenes on different surfaces and showed by comparison with an achiral counterpart that the presence of stereocenters is required to obtain helical aggregates.[10] Nevertheless, the way in which the chirality of conjugated oligothiophenes is transferred from the molecular level to supramolecular assemblies in thin films still remains unclear.

Some of us have recently reported on the use of the chiral 1,2-cyclohexandiamine scaffold (DACH)[11] to prepare a new family of chiral diamino-oligothiophenes as valuable ligands in palladium-catalyzed asymmetric transformations.[12] Triggered by their peculiar skeleton motifs, in which multiple specific active sites for noncovalent intra- and intermolecular interactions are present, we have now prepared oligothiophenes up to tetramers linked to chiral DACH spacers by diimine or diamine moieties and investigated the way stereochemical and spatial constraints imposed by DACH affect their self-organization in thin films.

We demonstrate that in these compounds the oligothiophene side arms adopt a helical arrangement both in solution and in the solid state, the overall handedness being dic-

[a] Dr. M. Melucci, Dr. G. Barbarella, Dr. M. Gazzano
Istituto per la Sintesi Organica e la Fotoreattività (ISOF)
Consiglio Nazionale Ricerche, Via Gobetti 101, 40129 Bologna (Italy)
Fax: (+39) 516-398-349
E-mail: mmelucci@isof.cnr.it

[b] Dr. M. Cavallini, Dr. F. Biscarini
Istituto per lo Studio dei Materiali Nanostrutturati ISMN-Sez Bo
Consiglio Nazionale Ricerche, Via Gobetti 101, 40129 Bologna (Italy)

[c] Prof. Dr. A. Bongini, Dr. F. Piccinelli, Prof. Dr. M. Monari, Dr. M. Bandini, Prof. Dr. A. Umani-Ronchi
Dipartimento di Chimica 'G. Ciamician'
Università di Bologna, via Selmi 2, 40126 Bologna (Italy)

[d] Prof. Dr. P. Biscarini
Dipartimento di Chimica Fisica e Inorganica
Università di Bologna, Viale Risorgimento 4, 40136 Bologna (Italy)

[**] DACH = *trans*-1,2-cyclohexanediamine.

Supporting information for this article is available on the WWW under http://www.chemeurj.org/ or from the author.

tated by the stereochemistry of DACH, the side-arm length, and the type of DACH–oligothiophene linker. We also show how these parameters are related to the morphology observed in cast films.

Results

Synthesis of chiral oligothiophenes: The synthesis of the diimino (DIT*n*) and diamino (DAT*n*) oligomers is summarized in Scheme 1. DIT*n* oligomers were obtained by condensing formylated oligothiophenes and commercial *R*,*R*, *S*,*S*, or racemic cyclohexanediamine (**1**) both by conventional heating and microwave-assisted processes.

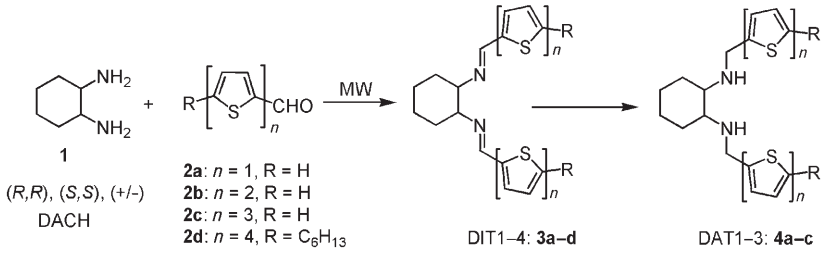

Scheme 1. Synthetic route to chiral DACH-linked oligothiophenes DIT*n* and DAT*n*.

Table 1 compares the results obtained with the two different procedures and shows that microwave (MW) heating reduces the reaction time from hours to minutes. This is particularly advantageous with longer oligothienyl systems, which need prolonged reaction times for complete conversion. A further advantage of the MW-assisted procedure comes from the fact that the desired products are obtained in high purity simply by filtration.

Table 1. Comparison between microwave irradiation and conventional heating in the synthesis of diimines **3a–d**.

Entry	**3**	MW heating[a]		Conventional heating[b]	
		Time [min]	Yield [%]	Time [h]	Yield [%]
1	**3a**	20	91	24	85
2	**3b**	20	70	24	70
3	**3c**	30	71	24	55
4	**3d**	30	48	48[c]	61

[a] All reactions were carried out in monochlorobenzene at 100 °C. [b] RT in CH_2Cl_2. [c] In CH_2Cl_2 under reflux.

The diamino derivatives DAT*n* were prepared by reduction of the corresponding DIT*n* using common hydride sources as previously described.[12] With thiophene and bithiophene diimine derivatives, $NaBH_4$ gave satisfactory results (88 and 75 % yields, respectively), while for the longer terthienyl derivative **3c**, $NaBH_3CN$ in the presence of dry HCl was needed to obtain the diamino derivative **4c** in reasonably good yield (44 % yield). However, to date, despite several attempts, we have not been able to achieve the reduction of **3d**.

Conformational analysis: To obtain information for use in aiding the analysis of experimental data, the conformational preferences of DIT*n* and DAT*n* were investigated using the semiempirical PM3 Hamiltonian which better describes the thiophene structure.[13]

For both families of compounds the orientation of the two arms can be either diequatorial or diaxial, and for each of them the possible rotations around the single bonds in the substituents have to be taken into account.

The calculations show that, as expected, the diimino derivatives are relatively rigid molecules. Only a few conformational families are populated with the diequatorial conformations being more stable than the diaxial ones by about 2 kcal mol^{-1}. Increasing the size of the arms does not alter the conformational profile of the system.

The diamino derivatives are much more flexible and several different conformations of similar energy are populated. The diequatorial conformational families are again energetically favored and, moreover, a strong tendency for the substituents to adopt a more compact structure was detected. The different conformational flexibility of the diimines and diamines is exemplified in Figure 1 in which the most stable calculated conformations of diimine (*R*,*R*)-DIT2 and diamine (*R*,*R*)-DAT2 are compared with the conformations present in single crystals (see also the X-ray section below). In both compounds the substituents are diequatorially oriented. Figure 1 shows that the conformation of the diimino compound that largely prevails in the calculated gas phase structure is very similar to the conformation present in the single-crystal X-ray structure. In contrast, the most stable

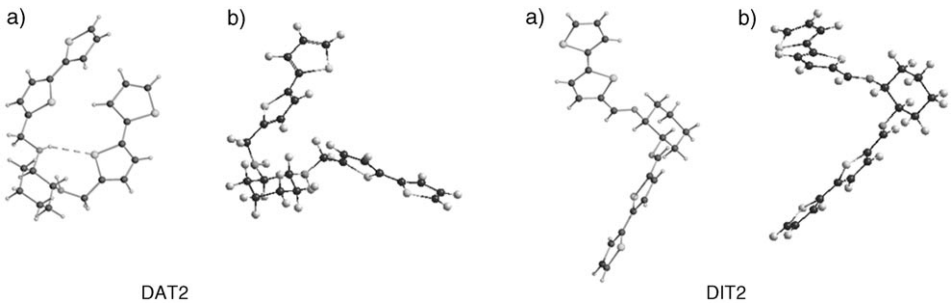

Figure 1. a) Crystallographic and b) calculated conformations of (*R*,*R*)-DAT2 and (*R*,*R*)-DIT2.

conformation of the diamino derivative in the gas phase, which is only slightly more populated than other geometrically similar conformations, differs considerably from that detected in the single crystal owing to packing interactions.

Chiroptical properties: In Figure 2 the UV/Vis and circular dichroism spectra of the diimines (*R*,*R*)-**3a–d** and diamines

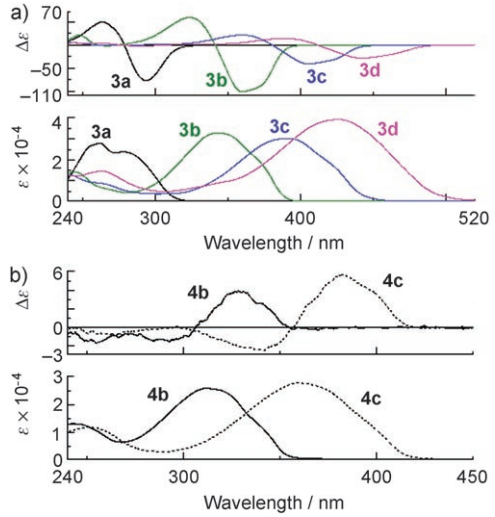

Figure 2. UV/Vis and CD spectra of diimines a) (*R*,*R*)-**3a–d** and b) diamines (*R*,*R*)-**4b,c** in chloroform. No appreciable CD signal was measured for (*R*,*R*)-**4a**.

(*R*,*R*)-**4b**,**c** in chloroform are reported. The values of maximum wavelength absorption (λ_{max}), molar absorbance (ε), molar CD ($\Delta\varepsilon$) or ellipticity (Ψ) of the Cotton peaks, and the chirality factor (g) for compounds **3a–d** and **4a–c** both in solution and as solid films are reported in the Supporting Information.

The wavelengths of maximum absorption for DIT*n* increase with the size of the oligothiophene arms as a result of the higher degree of delocalization in longer conjugated thienyl chains. As shown in Figure 2, the CD spectra of DIT*n* are characterized by a strong bisignated Cotton effect. According to the exciton coupling theory of Nakanishi and co-workers, the overall negative chirality observed for (*R*,*R*)-DIT*n* derives from the relative orientation and interaction of the two oligothiophene arms which are arranged in an *M* helical conformation (*M* helicity).[14]

Relative to the diimine precursors, the CD spectra of the diamines (*R*,*R*)-DAT*n* **4b,c** in chloroform showed much weaker bisignated Cotton effects and had an overall positive sign (*P* helicity, Figure 2). Also in these compounds the maximum wavelength absorption, corresponding to the crossover of the exciton couplet, was red-shifted on increasing the size of the oligothiophenes.

In marked contrast to the corresponding diimine **3a**, no CD signal was measured for the monothiophene diamine **4a** in the range of 240–500 nm.

Films of all these compounds on glass were prepared by casting a solution of a compound in chloroform (50 μL, $c \approx 10^{-3}$ M) and the corresponding CD spectra were recorded and compared with the solution spectra to provide information about changes in the conformational chirality in different phases.

The CD spectra of the cast films of (*R*,*R*)-DIT*n* (**3a–c**) showed no difference in shape with respect to those in solution (see the Supporting Information). The quarterthiophene derivative **3d**, being scarcely soluble in organic solvents, gave nonhomogeneous cast films. In this case, nonreproducible spectra were recorded.

Concerning the diamine derivatives, it was found that in the case of the (*R*,*R*)-diaminobithiophene **4b** the Cotton effect was opposite in sign to that in solution and showed an increased CD intensity over time, while for the diaminoterthiophene **4c** (DAT3) the Cotton effect had the same sign in solution as in the film and a markedly greater CD intensity was observed in the film spectrum (see the Supporting Information).

Figure 3 shows the CD spectra of diimine (*R*,*R*)-DIT2 (Figure 3a) in cast film and compares the CD spectra of diamine (*R*,*R*)-DAT2 in solution and in cast film (Figure 3b). In solution, (*R*,*R*)-DIT2 (Figure 2a) shows a bisignated Cotton effect with a negative Davydov component near $\lambda =$ 360 nm ($\Delta\varepsilon = -100.65$, chirality factor $g = -0.0037$) and a positive component near $\lambda = 324$ nm ($\Delta\varepsilon = +59.92$, $g = +0.0025$). The corresponding CD spectrum of the cast film was identical to that in solution with the negative and positive components at $\lambda = 366$ ($\Delta OD = -0.024$, $g = -0.025$) and 324 nm ($\Delta OD = +0.014$, $g = +0.011$), respectively. The spectrum did not vary over time, as observed for the other diimine derivatives.

In contrast, (*R*,*R*)-DAT2 in chloroform shows a bisignated CD spectrum with a positive component near $\lambda = 328$ nm ($\Delta\varepsilon = +3.96$, $g = +1.93 \times 10^{-4}$) and a negative component near $\lambda = 290$ nm ($\Delta\varepsilon = -1.55$, $g = -9.06 \times 10^{-5}$) (overall *P* helicity). On going from solution to film, DAT2 shows inversion of the Cotton effect with a negative component near $\lambda = 340$ nm ($\Delta OD = -0.0017$, $g = -0.0036$) and a positive component near $\lambda = 290$ nm ($\Delta OD = +0.00072$, $g = +0.0014$) indicating an overall negative chirality (*M* helicity). Thus, during the transition of DAT2 from solution to the solid state an inversion in relative orientations of the two chromophoric groups, corresponding to a helicity inversion, takes place.

Figure 3c shows the film spectra of (*R*,*R*)- and (*S*,*S*)-DAT2. As expected, the spectra show that the two compounds are enantiomeric. The fact that they show exactly the same profile, allows the presence of artefacts in the spectra to be excluded.[15]

Single-crystal X-ray structures of diimine DIT2 and diamine DAT2: (*R*,*R*)-Diimine DIT2 (**3b**) and (*R*,*R*)-diamine DAT2 (**4b**) yielded crystals suitable for X-ray diffraction studies. Figure 1 shows the single-crystal conformation of both compounds together with the corresponding preferred confor-

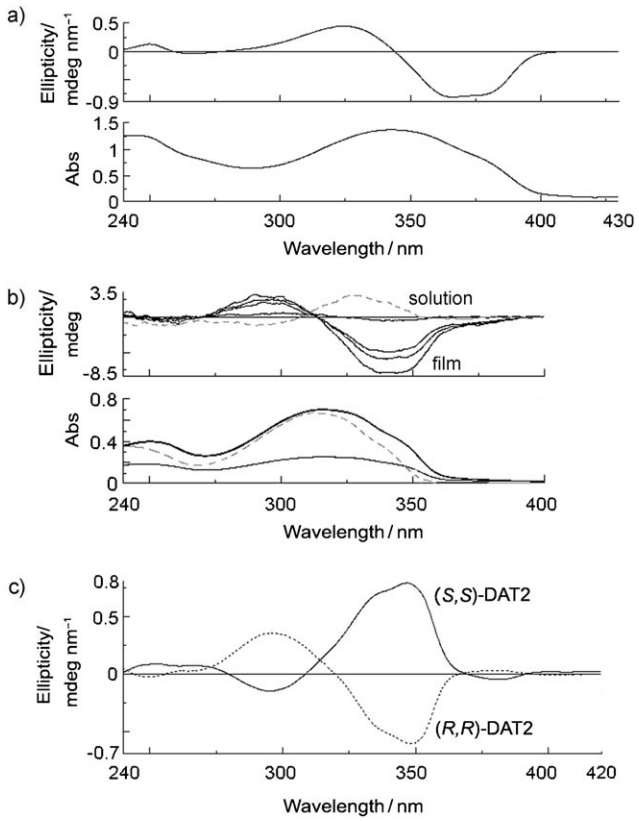

Figure 3. a) UV/Vis and CD spectra of (*R*,*R*)-DIT2 (**3b**) in cast film. b) UV/Vis and CD spectra of (*R*,*R*)-DAT2 (**4b**) in chloroform (dashed line) and in cast film (black line) and evolution over time of the CD amplitude in the cast film ($t = 10$, 30, 60 min; 3, 4 h). c) Comparison of the CD spectra of films of (*R*,*R*)- and (*S*,*S*)-DAT2 (**4b**). The ellipticity normalized for thickness and expressed in mdeg nm^{-1} is reported for spectra (a) and (c).

mations calculated for the gas phase.[16] In (*R*,*R*)-DIT2 (**3b**) the two bithiophene arms, which lie in the same plane as the imino groups, are perpendicular to each other and oriented in opposite directions. In contrast, the bithiophene arms of (*R*,*R*)-DAT2 (**4b**) approximately face each other so that the molecule assumes the shape of a small helicene. The X-ray structure of DAT2 reveals the presence of an intramolecular S···H–N interaction involving one inner sulfur atom and the amino hydrogen of the opposite pendant, as depicted in Figure 1.[17] Moreover, the crystal packing shows "slipped" π–π intermolecular stacking interactions along the *c* axis between thiophene rings of adjacent ribbons running along the *b* axis, which probably induces a lower crystal packing energy.

Thin-film characterization: The morphology of the diimine and diamine cast films was investigated by polarized optical microscopy and atomic force microscopy (AFM). Drop cast films of DIT1, DIT2, and DAT1 (both enantiomers) from chloroform were completely amorphous and smooth (root mean square (rms) roughness < 1 nm). Also, no sign of order was detected in cast films of DIT3, DAT3, and DIT4.

DAT2 was the only compound that gave highly crystalline cast films. For this compound it was possible to follow the film growth by joint optical microscopy, atomic force microscopy, and X-ray diffraction.

Optical microscopy displayed fast nucleation followed by growth with dendritic modalities resulting in triangular-shaped crystals over the entire substrate surface that exhibited birefringence. Figure 4 shows the polarized optical microscopy images of the film growth of (*R*,*R*)-DAT2 (**4b**). For comparison, we also studied the behavior of the racemic mixture of DAT2 (racemic DAT2) for which crystallization was markedly slower (a few hours vs a few minutes). In this case the crystallization resulted in the deposition of needle-shaped crystals of 100 μm length (Figure 4).[7b,18] After crystallization, the morphology becomes stable and does not change with the aging of the sample.

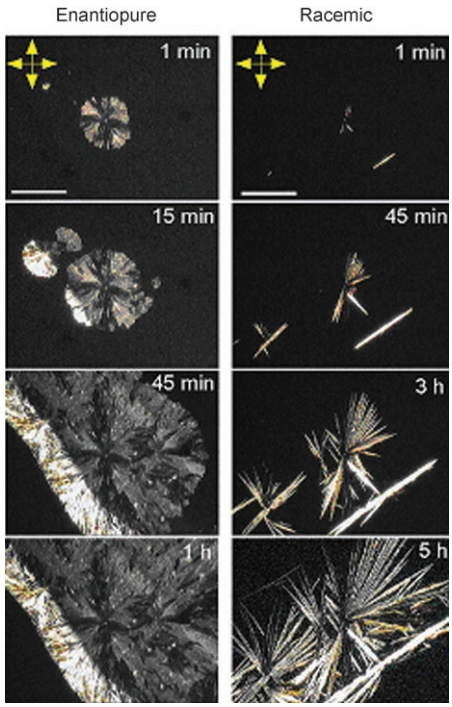

Figure 4. Optical micrographs with crossed polars of DAT2 film formation. The films were prepared by drop-casting on glass from 0.5 mM solutions in $CHCl_3$. The yellow arrows in the first row show the orientation of the crossed polars. The left column shows the evolution of enantiopure diamine (*R*,*R*)-DAT2, the right column the evolution of racemic DAT2.

The AFM images of enantiopure DAT2 (**4b**) films were consistent with optical microscopy observations as they showed the formation of an amorphous and very smooth film immediately after preparation evolving into a crystalline film within a few minutes (Figure 5). After complete crystallization of **4b**, crystals of dimensions ranging from micrometers to millimeters were observed in the film. They showed typical terrace structures with very flat terraces (rms roughness < 1 nm), the smallest step being of about 1.5 nm. Moreover some helicoidal structures (helicoids) with micro-

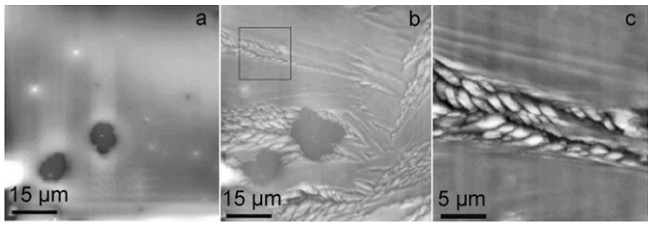

Figure 5. Evolution of the morphology of a cast film of diamine (*R*,*R*)-DAT2 (**4b**) on glass. The *Z* scale is 0–40 nm. a) Film morphology just after film preparation. b) Image acquired during the crystallization process. c) Detailed image of two helicoids formed during film crystallization. No influence of the AFM tip was observed in the morphology of crystallizing films.

metric dimensions were observed on the surface (Figure 5). The helicoids were formed during crystallization and optical microscopy showed birefringence, however, no extinguishment effects were observed by rotating the polars (on the contrary, the crystallites displayed some extinguishment according to optical anisotropic behavior of DAT2 crystals).

Although the helicoids seem to exhibit chirality (both left- and right-handed), no relationship with molecular chirality was observed.

The X-ray diffraction patterns of enantiopure and racemic DAT2 films (Figure 6) exhibited identical interplanar distances as well as molecular packing, indicating that chiral resolution of the racemate into homochiral crystals had taken place.[8c] Figure 6 shows the X-ray diffraction plots of enantiopure (*R*,*R*)- and racemic DAT2, together with the calculated X-ray diffraction profile of the former obtained by assuming a strongly preferred orientation of the 00*l* planes parallel to the substrate. The strong similarity between the experimental and calculated plots confirms that such an orientation is present in all samples. Some sketches of the structure of *(R*,*R*)-DAT2 with the *a*,*b* planes (00*l*) in contact with the glass surface are proposed in Figure 6.

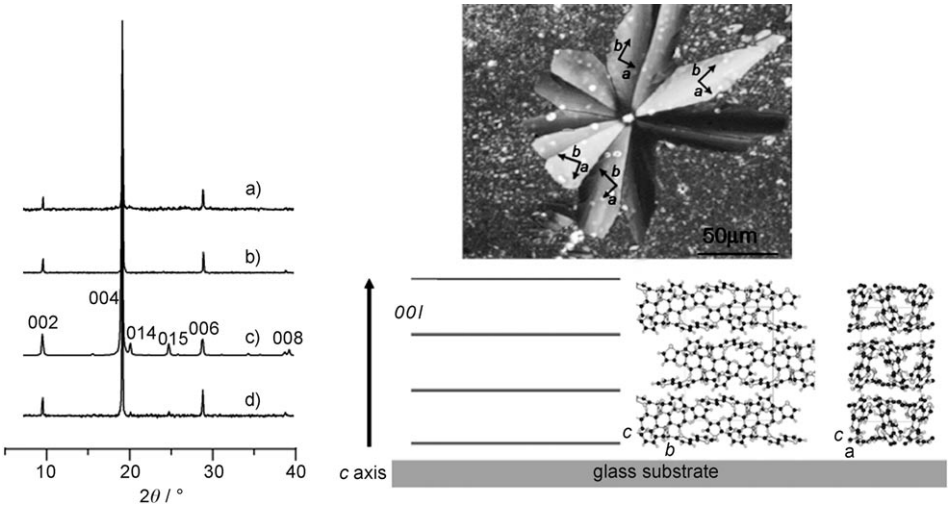

Figure 6. Left: XRD profile of racemic and enantiopure DAT2 drop cast films from chloroform. a) Racemic DAT2, b) (*S*,*S*)-DAT2, c) (*R*,*R*)-DAT2 calculated from the preferred orientation, and d) (*R*,*R*)-DAT2. The Miller indexes of the calculated peaks are reported. Right (bottom): Sketches of the organization of (*R*,*R*)-DAT2 molecules on a glass substrate. Two of the possible arrangements of the crystals are shown: the a,b plane is parallel to the substrate. Right (top): Crystalline film and possible arrangement of the crystallographic axes in the different domains.

Discussion

Our data show that the use of DACH scaffolds is a valuable way to obtain helical oligothiophene-based compounds with controllable helicity in solution. The helixlike conformation is maintained on increasing the size of the oligothiophene, indicating that DACH strongly acts to constrain the overall molecular structure. Switching of the helicity is achieved by changing the type of linker. For instance, the *M* helicity of diimines with *R*,*R* configuration turns to *P* helicity for diamines with the same absolute configuration, in accord with observations by Kwit and Gawronski for other diaryl-DACH derivatives.[11]

In solution, the intensity of the Cotton effect observed for diimines was significantly greater than that of the corresponding diamines. This effect can be rationalized through theoretical calculations which show that the C=N double bonds in diimine derivatives lead to conformational rigidity and to a highly preferred conformation, while in the diamine derivatives there are several geometrically different but almost isoenergetic conformations. In agreement with this, for diimine DIT2 the calculated structure is almost identical to that present in the single crystal, while in the case of diamine DAT2 the most stable conformation differs considerably from that detected in the crystal. In cast films the CD spectra of the diimine derivatives are similar to those observed in solution. Again, this result can be accounted for by the conformational rigidity of DIT*n*.

The CD signal from thin films of the more flexible diamino derivatives is remarkably more intense than that observed in solution.

The behavior of the enantiopure (*R*,*R*)- and (*S*,*S*)-diaminobis(bithiophenes) is unique, since for these compounds we observed the crystalline growth of the film, CD inversion, and chiral amplification on passing from solution to solid film.

In enantiopure DAT2 the helicity inversion from *P* to *M* helicity for the *R*,*R* configuration (or from *M* to *P* helicity for the *S*,*S* configuration) can be explained by assuming that (*R*,*R*)-**4b** exists in solution as an equilibrium of different conformational isomers with a slight preference for those with *P* helicity. Passing from solution to the solid film, a conformational change takes place leading to an *M* helical form,

which is stabilized by the intramolecular S···H interaction between the sulfur atom of one arm and the hydrogen atom of the N–H group of the opposite arm, as highlighted by single-crystal X-ray data. In turn, this conformational change is promoted by the minimization of the crystalline packing energy in the film. Note that intramolecular S···H–N hydrogen bonds have so far been reported only for thiaporphyrin systems[19] in which an appropriate orientation of atoms is imposed by the molecular geometry.

A working mechanism for helicity inversion in (*R*,*R*)-DAT2 is illustrated in Figure 7. During the transition from solution to amorphous solid to crystalline film, the *P* helical (*R*,*R*)-DAT2 conformers, which are slightly dominant in solution and in the solid amorphous phase, are progressively converted into the *M* helical conformers by rotation of the C–N bond of one arm.

The chiral amplification observed during film formation (see Figure 3b) can be ascribed to the increasing number of molecules characterized by *M* helicity with respect to those with *P* helicity during the 24 h required for complete film crystallization.

The kinetics for the growth of the cast film of racemic DAT2 are different to those of the enantiopure compounds, as shown in Figure 4, indicating that a chiral self-recognition process takes place between molecules with the same configuration. The occurrence of this chiral discrimination process is in agreement with the results obtained by X-ray diffraction of the films. Figure 6 shows that the same pattern is found for enantiopure and racemic compounds, confirming the deposition of homochiral crystals during the crystallization of the racemic form, as observed for many chiral conjugated molecules on solid surfaces.[8c]

On the basis of the experimental evidence presented here, it can be concluded that the peculiar behavior of enantiomeric pure diaminobis(bithiophene) can be rationalized in terms of conformational flexibility and a subtle interplay of intra- as well as intermolecular nonbonding interactions (i.e., hydrogen bonding, π stacking) involving both the chiral backbone and the oligothienyl pendants.

In contrast to DAT2, the shape of the CD spectrum of the cast film of the bis-terthiophene derivative DAT3 (**4c**) is very similar to that in solution, but is much more intense. For this compound it is likely that, despite the highly mobile C–N single-bond linker, the increased size of the pendants makes molecular rearrangements more difficult. However, the enhanced CD intensity observed for the cast films indicates that one preferred conformation exists in films.

Conclusion

In summary, we have presented new chiral helix-shaped oligothiophenes and demonstrated how the stereochemistry of DACH, the size of the side arms, and the type of DACH-oligothiophene linkers determine the conformational flexibility of these compounds and hence the overall handedness in solution and in solid film. In cast films these parameters are strictly related to supramolecular organization.

We have also demonstrated the detailed mechanism and the driving forces that in enantiopure diaminobis(bithiophene) DAT2 leads to the transfer of chirality from the molecular level in solution to the supramolecular level in film with inverted chirality. The peculiar case of this compound shows that noncovalent interactions in the solid state are crucial in determining thin-film properties. Such interactions, which play a major role in biological and supramolecular chemistry, should also be taken into account when designing new molecular materials for optical and electrical applications.

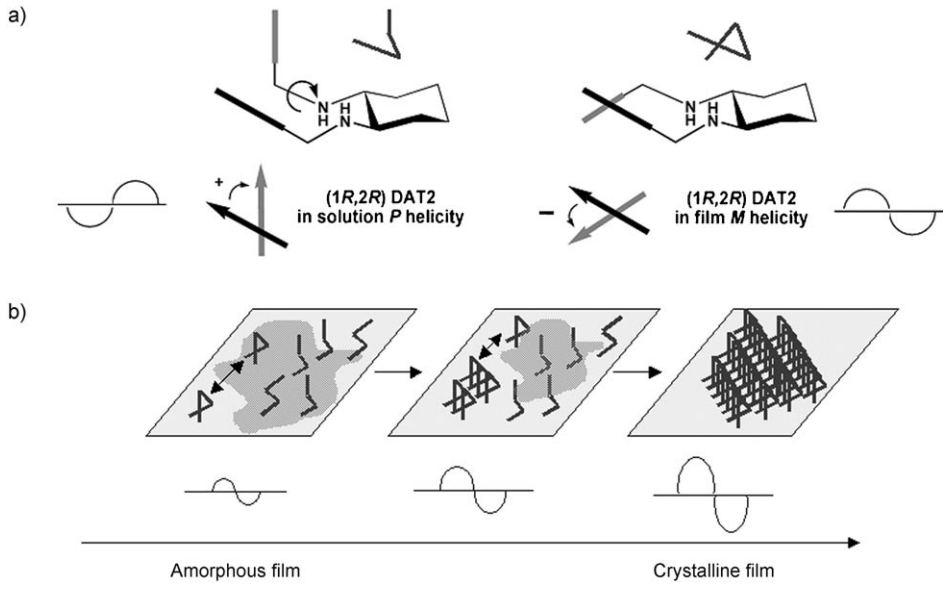

Figure 7. a) Schematic representation of the mechanism of helicity inversion for (*R*,*R*)-DAT2 (**4b**) from solution to thin film ascribable to a N–C bond rotation. b) Sketch of the bulk state transition for (*R*,*R*)-DAT2 from the amorphous to the crystalline phase.

Experimental Section

General: Microwave-assisted reactions were carried out in air using a commercial system, Synthewave 402 (Prolabo), with variable power and at a fixed temperature. Analytical thin-layer chromatography (TLC) was carried out by using 0.2 mm sheets of silica gel 60 F_{254} and visualization was accomplished with UV light (356 and 254 nm). UV/Vis and CD spectra were recorded with a JASCO J-810 spectropolarimeter under ambient conditions. A Nikon Eclipse 80i optical microscope was used for optical measurements. The images were re-

corded with a Nikon Coolpix 5400 digital color camera. Glass substrates were furnished by Knittel gläser and were washed with spectroscopic grade acetone (Aldrich) prior to use. Spectroscopic grade $CHCl_3$ (Aldrich) was used in solution preparation. Calculations were carried out by utilizing the HyperChem software package.[20] Melting points were determined by a Buchi-B540 and are uncorrected. IR analysis were performed with a FT-IR NICOLET 205 spectrophotometer and the spectra are expressed by wavenumber (cm^{-1}). Elemental analyses were carried out by using a EACE 1110 CHNOS analyzer. ^1H NMR and ^{13}C NMR spectra were recorded on a VARIAN-Mercury 400MHz spectrometer. Films were cast from a chloroform solution (~50 μL, $c \sim 10^{-3}$ M) on glass substrates and the solvent was evaporated under saturated atmosphere.

Crystal data were collected on a Bruker AXS CCD diffractometer ($Mo_{K\alpha}$ radiation, $\lambda = 0.71073$ Å). Empirical absorption correction was applied, initial structure model by direct methods, and anisotropic full-matrix least-squares refinement on F^2.

XRD measurements were carried out at room temperature with a Bragg/Brentano diffractometer (X'pertPro Panalytical) equipped with a graphite monochromator in the diffracted beam and by using a copper anode as the X-ray source. The simulated X-ray diffraction pattern was obtained by using the PowderCell program.[21]

Materials: 2,2′-Bithiophenyl-5-carbaldehyde (**2b**), enantiomerically pure (1*R*,2*R*)-1,2-diaminocyclohexane (**1**), and monochlorobenzene were obtained from Aldrich and used without further purification. The synthesis and characterization of aldehyde **2c** and diamines **4a–c** have already been described.[12a] 5‴-Hexyl-2,2′:5′,2″:5″,2‴-quarterthiophene-5-carbaldehyde (**2d**) was synthesized following a known procedure.[22]

(1*R*,2*R*)-*N*,*N*′-Bis(thiophen-2-ylmethylene)cyclohexane-1,2-diamine, DIT1 (3a): The microwave oven reactor was charged with thiophene-2-carbaldehyde (**2a**) (200 mg, 1.77 mmol), (1*R*,2*R*)-**1** (100 mg, 0.89 mmol), $MgSO_4$ (150 mg), and monochlorobenzene (1.5 mL). The mixture was irradiated for 10 min at 100 °C then further compound **1** (50 mg) was added and the mixture was irradiated for an additional 10 min at 100 °C. The $MgSO_4$ was filtered off and the solvent evaporated. The solid obtained was crystallized from *n*-hexane to gave DIT1 as a white solid (240 mg, 91 %). M.p. 120 °C; $[\alpha]_D = -23.6$ ($c = 0.64$ in $CHCl_3$); ^1H NMR ($CDCl_3$, 400 MHz): $\delta = 1.44$–1.50 (m, 2H), 1.78–1.85 (m, 6H), 3.30–3.33 (m, 2H), 6.96 (dd, $J = 3.6$, 4.8 Hz, 2H), 7.14 (d, $J = 4.0$ Hz, 2H), 7.29 (d, $J = 4.8$ Hz, 2H), 8.27 ppm (s, 2H); ^{13}C NMR ($CDCl_3$, 100 MHz): $\delta = 24.4$, 32.8, 73.4, 94.5, 127.2, 128.2, 130.2, 154.4 ppm; IR (Nujol): $\tilde{\nu} = 3383$, 3073, 2922, 2853, 1630, 1460, 1432, 1377, 1087, 716 cm^{-1}; UV/Vis (CH_2Cl_2): $\lambda_{abs} = 278$, $\lambda_{em} = 420$ nm; EI-MS: m/z: 112 (32), 160 (24), 193 (100), 302 (15) [$M^{\cdot+}$]; elemental analysis calcd for $C_{16}H_{18}N_2S_2$ (302.09): C 63.54, H 6.00, N 9.26; found: C 63.52, H 5.96, N 9.23.

(1*R*,2*R*)-*N*,*N*′-Bis(2,2′-bithiophenyl-5-ylmethylene)cyclohexane-1,2-diamine, DIT2 (3b): The microwave oven reactor was charged with 2,2′-bithiophenyl-5-carbaldehyde (**2b**) (180 mg, 0.91 mmol), compound **1** (52 mg, 0.46 mmol), $MgSO_4$ (50 mg), and monochlorobenzene (3 mL). The mixture was irradiated for 10 min then further **1** (26 mg, 0.23 mmol) was added. The mixture was irradiated for an additional 10 min and then the $MgSO_4$ was filtered off. After evaporating the solvent, the powder obtained was crystallized from isopropanol/pentane to gave DIT2 as a white powder (150 mg, 71 %). M.p. 136–137 °C; $[\alpha]_D = -1195$ ($c = 0.9$ in $CHCl_3$); ^1H NMR (C_6D_6, 400 MHz): $\delta = 1.20$–1.28 (m, 2H), 1.58–1.63 (m, 2H), 1.80 (brs, 4H), 3.22–3.28 (m, 2H), 6.49 (dd, $J = 3.6$, 5.2 Hz, 2H), 6.58–6.60 (m, 4H), 6.68 (d, $J = 4.0$ Hz, 2H), 6.89 (dd, $J = 0.8$, 3.6 Hz, 2H), 8.00 ppm (s, 2H); ^{13}C NMR (C_6D_6, 100 MHz): $\delta = 24.6$, 33.2, 73.7, 123.8, 124.5, 125.0, 128.7, 130.8, 137.6, 140.0, 142.0, 153.8 ppm; IR (Nujol): $\tilde{\nu} = 2922$, 2854, 1624, 1461, 1377, 791, 696 cm^{-1}; UV/Vis (CH_2Cl_2): $\lambda_{abs} = 345$, $\lambda_{em} = 447$ nm; EI-MS: m/z: 193 (100), 275 (80), 300 (50), 466 (20) [$M^{\cdot+}$]; elemental analysis calcd for ($C_{24}H_{22}N_2S_4$) (466.07): C 61.76, H 4.75, N 6.00; found: C 61.80, H 4.72, N 5.98.

(1*R*,2*R*)-*N*,*N*′-Bis(2,2′:5′,2″-terthiophen-5-ylmethylene)cyclohexane-1,2-diamine, DIT3 (3c): 2,2′:5′,2″-Terthiophene-5-carbaldehyde (**2c**) (170 mg, 0.62 mmol), diamine **1** (36 mg, 0.31 mmol), and $MgSO_4$ (180 mg) were dissolved in monochlorobenzene (4 mL) and introduced into a microwave oven reactor. After 15 min of irradiation at 100 °C further **1** (18 mg) was added and the mixture was irradiated for an additional 15 min. After filtration the solvent was evaporated and the solid was washed with warm isopropanol to gave DIT3 as a yellow solid (135 mg, 70 %). M.p. 146 °C; $[\alpha]_D = -830$ ($c = 1.01$ in $CHCl_3$); ^1H NMR ($CDCl_3$, 400 MHz): $\delta = 1.43$ (brs, 4H), 1.85 (brs, 4H), 3.37 (brs, 2H), 7.01–7.23 (m, 14H), 8.21 ppm (s, 2H); ^{13}C NMR ($CDCl_3$, 100 MHz): $\delta = 24.4$, 32.8, 73.4, 123.4, 123.9, 124.4, 124.7, 125.0, 127.9, 131.0, 135.9, 136.9, 137.0, 139.5, 140.9, 154.1 ppm; IR (Nujol): $\tilde{\nu} = 2853$, 2726, 1623, 1461, 1377, 792 cm^{-1}; UV/Vis (CH_2Cl_2): $\lambda_{abs} = 390$, $\lambda_{em} = 477$ nm; EI-MS: m/z: 149 (10), 275 (100), 357 (28), 382 (21), 630 (11) [$M^{\cdot+}$]; elemental analysis calcd for $C_{32}H_{26}N_2S_6$ (630.04): C 60.91, H 4.15, N 4.44; found: C 60.85, H 4.12, N 4.42.

(1*R*,2*R*)-*N*,*N*′-Bis(5‴-hexyl-2,2′:5′,2″:5″,2‴-quarterthiophen-5-ylmethylene)cyclohexane-1,2-diamine, DIT4 (3d): Aldehyde **2d** (500 mg, 1.13 mmol) and diamine **1** (65 mg, 0.57 mmol) were dissolved in monochlorobenzene (15 mL) and introduced into a microwave oven reactor. The mixture was irradiated for 40 min at 100 °C and then cooled to room temperature. The precipitate formed was filtered and then washed with warm *n*-hexane affording diimine **9** (350 mg, 64 %) as an orange powder. M.p. 193 °C; $[\alpha]_D = -1895$ ($c = 0.2$ in CH_2Cl_2); ^1H NMR ($CDCl_3$, 400 MHz): $\delta = 0.90$ (brs, 6H), 1.61 (m, 24H), 2.80 (m, 4H), 3.20 (brs, 2H), 6.69 (s, 2H), 7.04 (m, 14H), 8.22 ppm (s, 2H); ^{13}C NMR ($CDCl_3$, 100 MHz): $\delta = 14.0$, 22.6, 24.4, 28.7, 30.2, 31.5, 32.8, 73.41, 123.5, 124.1, 124.5, 124.9, 125.1, 131.2, 134.3, 134.9, 135.7, 136.9, 137.2, 139.5, 145.8, 154.1 ppm; IR (Nujol): $\tilde{\nu} = 2852$, 2780, 1623, 1460, 1377, 791 cm^{-1}; UV/Vis (CH_2Cl_2): $\lambda_{abs} = 420$, $\lambda_{em} = 510$ nm; EI-MS: (m/z): 441, 482; elemental analysis calcd for $C_{52}H_{54}N_2S_8$ (963.21): C 64.82, H 5.65, N 2.91; found: C 64.78, H 5.60, N 2.90.

Acknowledgements

This work was supported by projects EU-NMP-IP 500355 NAIMO, Marie Curie RTN CHEXTAN and FIRB RBNE03S7XZ_005. Thanks are due to Dr. Maria Antonietta Loi (Istituto per lo Studio dei Materiali Nanostrutturati ISMN-Sez Bo, CNR, Italy) for the optical and fluorescence microscopy images of enantiopure and racemic DAT2 **4b**.

[1] G. Barbarella, M. Melucci, G. Sotgiu, *Adv. Mater.* **2005**, *17*, 1581–1593.

[2] a) H. Sirringhaus, *Adv. Mater.* **2005**, *17*, 2411–2425; b) G. Witte, C. Wöll, *J. Mater. Res.* **2004**, *19*, 1889–1916; c) C. D. Dimitrakopoulos, P. R. L. Malenfant, *Adv. Mater.* **2002**, *14*, 99–117; d) H. Hoppe, N. S. Sariciftci, *J. Mater. Res.* **2004**, *19*, 1924–1945; e) A. Köler, J. S. R. Wilson, H. Friend, *Adv. Mater.* **2002**, *14*, 701–707.

[3] F. Dinelli, M. Murgia, F. Biscarini, D. M. De Leeuw, *Synth. Met.* **2004**, *146*, 373–376.

[4] R. Garcia, M. Tello, *Nano Lett.* **2004**, *4*, 1115–1119.

[5] G. Derue, S. Coppèe, S. Gabriele, M. Surin, V. Geskin, F. Monteverde, P. Leclère, R. Lazzaroni, P. Damman, *J. Am. Chem. Soc.* **2005**, *127*, 8018–8019.

[6] F. Dinelli, M. Murgia, P. Levy, M. Cavallini, F. Biscarini, D. M. De Leeuw, *Phys. Rev. Lett.* **2004**, *92*, 116802-1.

[7] a) A. T. ten Cate, P. Y. W. Dankers, H. Kooijman, A. L. Spek, R. P. Sijbesma, E. W. Meijer, *J. Am. Chem. Soc.* **2003**, *125*, 6860–6861; b) A. P. H. J. Schenning, A. F. M. Kilbinger, F. Biscarini, M. Cavallini, H. J. Cooper, P. J. Derrick, M. J. Feast, R. Lazzaroni, Ph. Leclère, L. A. McDonell, E. W. Meijer, S. C. J. Meskers, *J. Am. Chem. Soc.* **2002**, *124*, 1269–1275; c) D. Beljonne, B. M. W. Langeveld-Voss, Z. Shuai, R. A. J. Janssen, S. C. J. Mekers, E. W. Meijer, J. L. Bredas, *Synth. Met.* **1999**, 912–913.

[8] a) A. Miura, P. Jonkeijm, S. De Feyter, A. P. H. J. Schenning, E. W. Meijer, F. C. De Schryver *Small*, **2005**, *1*, 131–137; b) M. C. Blüm, E. Æavar, M. Pivetta, F. Patthey, W. D. Schneider, *Angew. Chem.* **2005**, *117*, 5468–5471; *Angew. Chem. Int. Ed. Engl.* **2005**, *44*, 5334–5337; c) W. Mamdouh, H. Uji-i, A. E. Dulcey, V. Percec, S. De Feyter, F. C. De Schryver, *Langmuir* **2004**, *20*, 7678–7685; d) S. M. Barlow, S. Louafi, D. Le Roux, J. Williams, C. Muryn, S. Haq, R.

Raval, *Langmuir* **2004**, *20*, 7171–7176; e) S. De Feyter, A. Gesquière, K. Wurst, D. S. Amabilino, J. Veciana, F. C. De Schryver, *Angew. Chem.* **2001**, *113*, 3317–3320; *Angew. Chem. Int. Ed.* **2001**, *40*, 3217–3220; f) A. Gesquière, P. Jonkheijm, F. J. M. Hoeben, A. P. H. J. Schenning, S. De Feyter, F. C. DeSchryver, E. W. Meijer, *Nano Lett.* **2004**, *4*, 1175–1179; g) M. Miyasaka, A. Rajca, M. Pink, S. Rajca, *Chem. Eur. J.* **2004**, *10*, 6531–6539; h) A. Gesquière, M. M. Abdel-Mottaleb, S. De Feyter, F. C. De Schryver, F. Schoonbeek, J. van Esch, R. M. Kellogg, B. L. Feringa, A. Calderone, R. Lazzaroni, J. L. Brédas, *Langmuir* **2000**, *16*, 10385–10391.

[9] a) E. L. Eliel, S. H. Wilen, *Stereochemistry of Organic Compounds*, Wiley, New York, **1994**; b) R. Fasel, M. Parschau, K. H. Ernst, *Nature* **2006**, *439*, 449–452; c) F. J. M. Hoeben, P. Jonkheijm, E. W. Meijer A. P. H. J. Schenning, *Chem. Rev.* **2005**, *105*, 1491–1546; d) J. J. L. M. Cornelissen, A. E. Rowan, R. J. M. Nolte, N. A. J. M. Sommerdijk, *Chem. Rev.* **2001**, *101*, 4039–4070.

[10] P. Leclère, M. Surin, R. Lazzaroni, A. F. M. Kilbinger, O. Henze, P. Jonkheijm, F. Biscarini, M. Cavallini, W. J. Feast, E. W. Meijer, A. P. H. J. Schenning, *J. Mater. Chem.* **2004**, *14*, 1959–1963.

[11] M. Kwit, J. Gawronski, *Tetrahedron* **2003**, *59*, 9323–9331.

[12] a) V. G. Albano, M. Bandini, M. Melucci, M. Monari, F. Piccinelli, S. Tommasi, A. Umani-Ronchi, *Adv. Synth. Catal.* **2005**, *347*, 1507–1512; b) V. G. Albano, M. Bandini, G. Barbarella, M. Melucci, M. Monari, F. Piccinelli, S. Tommasi, A. Umani-Ronchi, *Chem. Eur. J.* **2006**, *12*, 667–676.

[13] J. J. P. Stewart, *J. Comput. Chem.* **1989**, *10*, 209–220.

[14] a) N. Harada, K. Nakanishi, *Circular Dichroic Spectroscopy: Exciton Coupling in Organic Stereochemistry*, University Science Books, Mill Valley, CA, **1983**; b) N. Ikemoto, I. Estevez, K. Nakanishi, N. Berova, *Heterocycles* **1997**, *46*, 489–501.

[15] Artefacts due to linear dichroism can be excluded by considering the LD low values measured ($\approx 10^{-3}$). The spectra were also reproducible after substrate rotation. *Circular Dichroism* (Eds.: N. Berova, K. Nakanishi, R. W. Woody), Wiley, New York, **2000**, p. 159.

[16] Crystal data were collected on a Bruker AXS CCD diffractometer ($Mo_{K\alpha}$ radiation, $\lambda = 0.71073$ Å): Empirical absorption correction applied, initial structure model by direct methods and anisotropic full-matrix least-squares refinement on F^2. Data for DAT2: $C_{24}H_{26}N_2S_4$; $M_r = 470.71$; orthorhombic $P2_12_12_1$; $a = 9.144(4)$, $b = 14.195(7)$, $c = 18.624(9)$ Å; $V = 2417(2)$ Å^3; $Z = 4$; $D_x = 1.293$ Mg m^{-3}; $\mu = 0.407$ mm^{-1}; $F(000) = 992$; $T = 293(2)$ K; $\theta_{max} = 23.25°$; 6141 reflections; 1029 $I > 2\sigma(I)$. Final indices: $R_1 = 0.0822$, $wR_2 = 0.1419$. GOF = 0.848, absolute structure parameter = −0.2(3). Data for DIT2: $C_{24}H_{22}N_2S_4$; $M_r = 466.68$; tetragonal $P4_12_12$; $a = 6.2940(4)$, $b = 6.2940(4)$, $c = 58.515(4)$ Å; $V = 2318.0(3)$ Å^3; $Z = 4$; $D_x = 1.337$ Mg m^{-3}; $\mu = 0.424$ mm^{-1}; $F(000) = 976$; $T = 293(2)$ K; $\theta_{max} = 28.01°$; 21459 reflections; 2473 $I > 2\sigma(I)$. Final indices: $R_1 = 0.0714$, $wR_2 = 0.1631$. GOF = 1.143, absolute structure parameter = 0.2(2). CCDC-275638 (DAT2, **4b**) and CCDC-275639 (DIT2, **3b**) contain the supplementary crystallographic data for this paper. These data can be obtained free of charge from the Cambridge Crystallographic Data Centre via www.ccdc.cam.ac.uk/data_request/cif.

[17] F. A. Hallen, C. M. Bird, R. S. Rowland, P. R. Raithby, *Acta Crystallogr., Sect. B* **1997**, *53*, 680–695.

[18] B. M. W. Langeveld-Voss, D. Beljonne, Z. Shuai, R. A. J. Janssen, S. C. J. Meskers, E. W. Meijer, J.-L. Brédas, *Adv. Mater.* **1998**, *10*, 1343–1348.

[19] a) S. J. Narayanan, B. Sridevi, T. K. Chandrashekar, A. Vij, R. Roy, *J. Am. Chem. Soc.* **1999**, *121*, 9053–9068; b) S. J. Narayanan, B. Sridevi, T. K. Chandrashekar, A. Vij, R. Roy, *Angew. Chem.* **1998**, *110*, 3582–3585; *Angew. Chem. Int. Ed.* **1998**, *37*, 3394–3397; c) N. Agarwal, C.-H. Hung, M. Ravikanth, *Eur. J. Org. Chem.* **2003**, 3730–3734; d) V. G. Anand, S. K. Pushpan, S. Venkatraman, A. Dey, T. K. Chandrashekar, B. S. Joshi, R. Roy, W. Teng, K. R. Senge, *J. Am. Chem. Soc.* **2001**, *123*, 8620–8621.

[20] HyperChem rel. 7.0, Windows Molecular Modeling System, HyperCube, Inc and Autodesk Inc, developed by HyperCube, Waterloo, Ontario, Canada, **1993**.

[21] PowderCell for Windows, W. Kraus, G. Nolze, Federal Institute for Materials and Testing (BAM), Berlin, Germany, version 2.3, **1999**.

[22] M. Melucci, G. Barbarella, M. Zambianchi, M. Benzi, F. Biscarini, M. Cavallini, A. Bongini, S. Fabbroni, M. Mazzeo, M. Anni, G. Gigli, *Macromolecules* **2004**, *37*, 5692–5702.

Received: March 6, 2006

